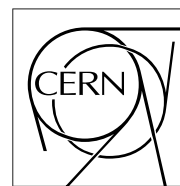


The Compact Muon Solenoid Experiment

# CMS Note

Mailing address: CMS CERN, CH-1211 GENEVA 23, Switzerland



June 26, 1998

## Test results of a MSGC detector module for the CMS forward MSGC-Tracker

M. Kräber, P. Blüm, K.Kärcher, D. Knoblauch, R. Metri, Th. Müller, D. Neuberger, A. Pallarès<sup>a)</sup>,  
H.J. Simonis, W.H. Thümmel.

*Institut für Experimentelle Kernphysik, Universität Karlsruhe*

### Abstract

We report on the construction and test beam results of a MSGC detector module with four trapezoidal elements arranged in a geometry as planned for the CMS forward tracker. Our objective is to study a concept for the forward detector modules which is easy to build with minimal contribution to the material budget. Signal to noise ratio and spatial resolution of the detector are studied for different bias voltages in a 100 GeV muon beam at CERN.

---

<sup>a)</sup> *Corresponding author*

# 1 Introduction

MicroStrip Gas Chambers (MSGC) are foreseen as one of the key detectors of the CMS tracking system. Detector modules have to be designed as well for the tracker barrel as for the forward region. The module which is described here is dedicated to the forward region. It is a closed system of four trapezoidal detector units mounted together in a segment of a ring (called detector module) with the read-out electronics and high voltage connections outside of the gas volume of the detector.

## 2 Concept of the detector module : *the Euro-banana*

### 2.1 Detector description

The module is designed for 4 wedge shaped MSGC substrates with 512 readout channels each. In the test module, to save expenses, only the 2 central substrates are real detectors, the remaining ones are bare glass plates. DESAG D263 glass, 200  $\mu\text{m}$  thick, is used for the substrates. A detailed description can be found in [1].

#### 2.1.1 Strip structure

Anode and cathode structure are engraved into a 500 nm thick aluminium layer. The lithography was done by Optimask<sup>1)</sup>. On each substrate, 512 anodes, 10  $\mu\text{m}$  wide, 121.51 mm long, are interleaved with cathode strips with a width ranging from 84.7 to 100  $\mu\text{m}$ . The resulting pitch varies from 200 to 179.9  $\mu\text{m}$  to guarantee uniform gain along the strips [2].

Anodes can be read out individually while cathodes are grouped together in 31 blocks of 16 and one block of 17 cathodes strips.

#### 2.1.2 Drift cathode

The individual drift cathodes are made of 200  $\mu\text{m}$  thick DESAG D263 on which a 5 nm chromium layer was evaporated. The drift cathodes remain optically semi-transparent.

The outer drift planes of the detector module are bare glass plates facing the dummy substrates.

#### 2.1.3 Frame

The module frame is mainly made of glass tubes (inner radius : 2.6 mm, outer radius : 3.3 mm) which provide a simple way for the gas supply. Two tubes on opposite sides of the frame contain small holes (250  $\mu\text{m}$  diameter) to allow gas flow in and out of the detector volume.

Angular connectors to the glass tubes are made of Stesalit<sup>2)</sup>. They are glued together with the glass tubes on a Stesalit gluing jig using Epotec H72 thermally hardening glue (see figure 1). This provides a clean and cheap solution (about 50 DM) for the module frame.

#### 2.1.4 Burst protection

In order to protect the delicate glass plates, a “gravity” controlled gas by-pass line to the module is installed. Mainly made of stainless steel, the by-pass opens as soon as the pressure in the module exceeds 2.5 mbar. This makes a gas feed-back system over the surfaces unnecessary and guarantees a minimal load to the material budget [3].

## 2.2 Mounting

Before mounting, all elements are cleaned in an ultrasonic bath with deionized water, followed by a bath in isopropanol and a subsequent drying procedure.

A more complicated bath sequence is used to clean substrates and drift cathodes : 20 min ultrasonic deionized water bath, 10 min acetone bath, flush under deionized water, 10 min isopropanol bath, flush under deionized water and drying with nitrogen (procedure suggested by IMT<sup>3)</sup> ).

---

<sup>1)</sup> Optimask, Paris, France.

<sup>2)</sup> Stesalit AG, Zullwill, Switzerland.

Substrates, frame and drift cathodes are glued together with Epotec H72. The substrates are aligned to each other with a precision better than  $50\ \mu\text{m}$  using a coordinate machine.

Finally, all  $\Phi$ -cracks (space between 2 substrates) are sealed by gluing a  $100\ \mu\text{m}$  thin DESAG 263 glass strip on the outside of the detector (leakage rate is measured to be less than 2% of the total gas volume).

## 2.3 Connections

### 2.3.1 High voltage connections

All the connection pads are outside of the gas volume of the detector. Connection to drift cathodes is made by gluing with conductive silver. Araldit passivation is applied on the remaining metallized structure to avoid discharges. Cathode groups are wire-bonded to a pitch adaptor. This adaptor is connected to a high voltage hybrid with  $1\ \text{M}\Omega$  resistors for each group of 16 cathode strips preceded by a common  $10\ \text{M}\Omega$  protection resistor.

### 2.3.2 Read-out electronics

To allow easy exchange of the read-out electronics, a combination of usual bonding and anisotropic conductive film gluing is used. A kapton foil with  $100\ \mu\text{m}$  wide copper strips ( $200\ \mu\text{m}$  pitch) is glued under the substrate, another one under the read-out electronics. Anodes and read-out electronics are bonded to those foils. A third kapton foil was glued on the two foils using Elatech anisotrop R008 conductive film to connect anodes to electronics (see figure 2).

During laboratory test, Preshape32 chips were used. Inconvenient is that one separate ADC channel is required for each strip.

For the test beam, multiplexed Premux128 [4] chips are used. A Premux chip contains 128 channels of charge preamplifiers and shaper-amplifiers plus 128 channels of double-correlated sampling circuitry and an analogue multiplexer. With some additional circuitry (motherboard) to handle the token-passing and output buffering a single Flash-ADC board channel is sufficient to read-out an entire detector module. A motherboard, containing 4 Premux128 chips, is connected to the 512 central strips.

## 3 Test beam set-up

The set-up of the beam test performed in August '97 in the X5 beam line of the CERN SPS West Area is shown in figure 3.

A trigger on the 100 GeV muon beam was obtained by the coincidence of 2 plastic scintillators, of dimensions  $10\times 10$  and  $2\times 2\ \text{cm}^2$ , respectively.

Silicon detectors of known performances were used as reference telescope [5] to reconstruct the trajectories of incoming particles. They were grouped as B1 and B2. Each consist of 2 identical double-sided silicon microstrip detectors with orthogonal strips of area  $1.92\times 1.92\ \text{cm}^2$  and thickness  $300\ \mu\text{m}$ . Each plane has 384 read-out strips with  $50\ \mu\text{m}$  pitch on each side.

The MSGC detector module was sitting on the same optical bench as the second telescope module. Between the 2 telescope modules was an optical bench supporting various silicon detectors for test.

## 4 Data acquisition system

A new multi-crate DAQ system was developed for the CMS tracker milestones [6] where all detectors were equipped with Premux128 electronics. The read-out sequence was generated by a VME sequencer and the ADC sampling was done by VME Sirocco II modules.

The front-end crates used FIC 8243/43 for data pre-processing. Communications between the front-end crates and the event builder crate were protocolled over a VIC 8251 bus. The event builder is VME based Lynx-OS RTPC 8067 which handled the reconstruction of Zebra banks. In final Zebra structure, data were sent to a Sun Themis to handle the logging to tape at the CERN main control room and, partially (about 50 events per spill), to a Sun work-station for on-line monitoring.

---

<sup>3)</sup> IMT AG, Im Langacher, Greifensee, Switzerland.

## 5 Offline analysis

The off-line analysis is done by means of a program developed by the CMS collaboration [7].

### 5.1 Cluster finding

The *ADC* raw data for strip  $i$  for event  $k$  is the sum of 3 components :

$$ADC^k(i) = S^k(i) + PED^k(i) + CM^k(i)$$

$S^k(i)$  is the ionization signal seen on strip  $i$  at event  $k$ .  $PED^k(i)$  is the strip pedestal and  $CM^k(i)$  the common mode shift for event  $k$ .

The pedestal of each strip is defined as average of the *ADC* counts of that channel, evaluated and updated every 100 events, taking care to exclude events where this strip has recorded a particle hit. Using the same sample of 100 events the strip noise  $N^k(i)$  as the statistical fluctuation of the signal  $S^k(i)$  is also calculated. The first 50 events are used to calculate the starting values for pedestal and noise for each channel.

The off-line algorithm is looking for neighbouring strips satisfying  $S(i)/N(i) > T_0$  with  $T_0 = 7$ . Once at least one such strip is found, all adjacent strips with  $S(j)/N(j) > T_1$  with  $T_1 = 3$  are added to form a cluster. When no more adjacent strips are found, the cluster charge  $S_{cluster}$  is defined as the sum of the signals over a group of accepted strips.

The cluster noise is computed as :

$$N_{cluster} = \sqrt{\sum_{cluster} N(i)^2 / L_{cluster}}$$

where  $L_{cluster}$  is the number of strips accepted in that cluster. If the condition  $S_{cluster}/N_{cluster} > T_2$  where  $T_2 = 3$  is satisfied, the cluster is retained. The position of the cluster is calculated as the center of gravity of pulse height weighted strips in the cluster.

### 5.2 Tracking

The trajectory of an incoming particle is reconstructed with the help of 2 telescope planes.

Particle hits in the first and the last telescope detector determine coordinates in the  $x$  and  $y$  direction. Straight lines for each direction are extrapolated to determine the probable impact point on the detector plane.

A common coordinate system is defined for the 2 telescope planes. In each direction,  $x''$  and  $y''$ , the line corresponding to the particle trajectory is defined.

This coordinate system is rotated to be aligned with the plane of the detector under study. The rotation angle  $-\alpha$  is determined by a global minimization of the width of the residual distribution (see figure 4).

This defines a new  $x', y'$  coordinate system. This latter system has to be shifted to be aligned with the  $x$  axis of the detector plane as shown by figure 5. Extrapolated cluster position is then expressed in polar coordinates (the crossing point of all strips is given as origin of this system). So, from information given by the telescope (see figure 6), the particle is expected at :

$$r_{tel} = \sqrt{(x + \Delta x)^2 + y^2}$$

$$\phi_{tel} = \arctan \frac{y}{x + \Delta x}$$

Only angular information,  $\phi_{msgc}$  is given by the MSGC plane. The radial coordinate is assumed to be equivalent to radial information given by the telescope. The position of the center of gravity of the largest cluster,  $c$ , is known in strip coordinates. Angle  $\phi$  between strips is constant.

$$\phi_{msgc} = \phi \times c$$

Finally, the residual distribution is given by :

$$res = r_{tel} \times \sin(\phi_{msgc} - \phi_{tel})$$

## 6 Results

### 6.1 Charge response and signal to noise ratio

A typical detector response is given by the set of plots of figure 7. These plots refer to perpendicular tracks with cathode voltage  $V_{cath} = -520$  V and drift voltage  $V_{drift} = -2700$  V with a neon/DME (1/2) gas mixture.

The position of the center of gravity of the largest cluster is given in figure 7a and shows where the beam hits the chamber.

The distribution of the signal is shown in figure 7b. The distribution of the total charge collected in a cluster can be fitted by a Landau function as shown on the plot.

The cluster noise and signal to noise ratio, as defined previously, are shown figure 7c and 7d.

The number of strips per cluster is given by plot 7e. One can see that the charge of the cluster is mainly, about 75%, shared by 2 or 3 strips.

The cluster multiplicity is a measure of how many clusters are found in an event (see figure 7f). Most of the time only one cluster is found.

### 6.2 Bias voltage scan

A voltage scan study was done to evaluate the effect of bias voltage on the signal to noise ratio. We observe only small variations of cluster noise. With the signal also the signal to noise ratio increases. Figure 8 shows the ratio of the most probable signal value from the Landau fit divided by the average noise value given by a Gaussian fit.

### 6.3 Resolution and tracking efficiency

Figure 9a shows the typical difference between the hit position extrapolated by the telescope and the hit position given by the MSGC as a function of  $x$ . The plotted 2 cm zone is correlated to the dimension of the telescope silicon detectors.

When the residual is plotted as a function of strip number, one can recognize the MSGC strip structure as shown in figure 9b. Broken strips cause clear disturbance in the residual distribution. Without cuts on bad regions, the spatial resolution of the MSGC module is estimated at  $33.6 \mu\text{m}$ . After excluding bad regions containing broken strips, the spatial resolution is  $26.3 \mu\text{m}$  (see figure 10).

We defined tracking efficiency as the ratio of hits seen in the MSGC which have a maximal  $200 \mu\text{m}$  deviation from the hit position predicted by the telescope and the total number of particle tracks seen by the telescope. Due to a poor substrate quality (more than 50% broken strips), tracking efficiency is rather low, increasing slightly with cathode voltage as shown figure 11. Calculated for the whole detector, the mean value of tracking efficiency is 70%. If restricted to regions of the detector with no missing strips, the tracking efficiency is 98.1% for a cathode voltage of  $V_{cath} = -520$  V.

## 7 Conclusions

This paper describes the concept of a closed MSGC detector module comprising 4 wedge shaped substrates. Particular emphasis is given to develop a simple and inexpensive (50 DM) mechanical assembly method providing a minimal contribution to the material budget of the CMS tracker ( $1.5 \times 10^{-3} \text{ g/mm}^{-2}$ ). The detector has been tested in a 100 GeV muon beam at Cern. The spatial resolution has been measured to be  $26.3 \mu\text{m}$  using the center of gravity of the energy deposit. The tracking efficiency was found to be 98%.

## References

- [1] M. Kräber, *Bau und Test eines Prototypen für den Vorwärts-CMS-Spurdetektor*, Diplomarbeit, Universität Karlsruhe - Institut für Experimentelle Kernphysik, 1998.
- [2] **CMS Technical Proposal**, CERN/LHCC 94-38.
- [3] S. Bachmann et al., **CMS Note 1997/063**, *Beam test performance of a closed microstrip gas chamber module for the CMS forward tracker*,

- [4] L.L. Jones, **Premux specification**, Version 2.3, January 1995.
- [5] L. Celano et al., **Nucl. Instr. and Meth. A 381 (1996) 49-56** "A high resolution beam telescope built with double sided silicon strip detectors".
- [6] B. Schwaller et al., **Proceedings of IEEE Nuclear Science Symposium and Medical Imaging Conference 97** " A unix SVR4-OS9 distributed data acquisition for high energy physics".
- [7] O. Adriani et al. **CMS Note 1997/006**, "Beam test results for single and double sided silicon detector prototypes of the CMS central detector".

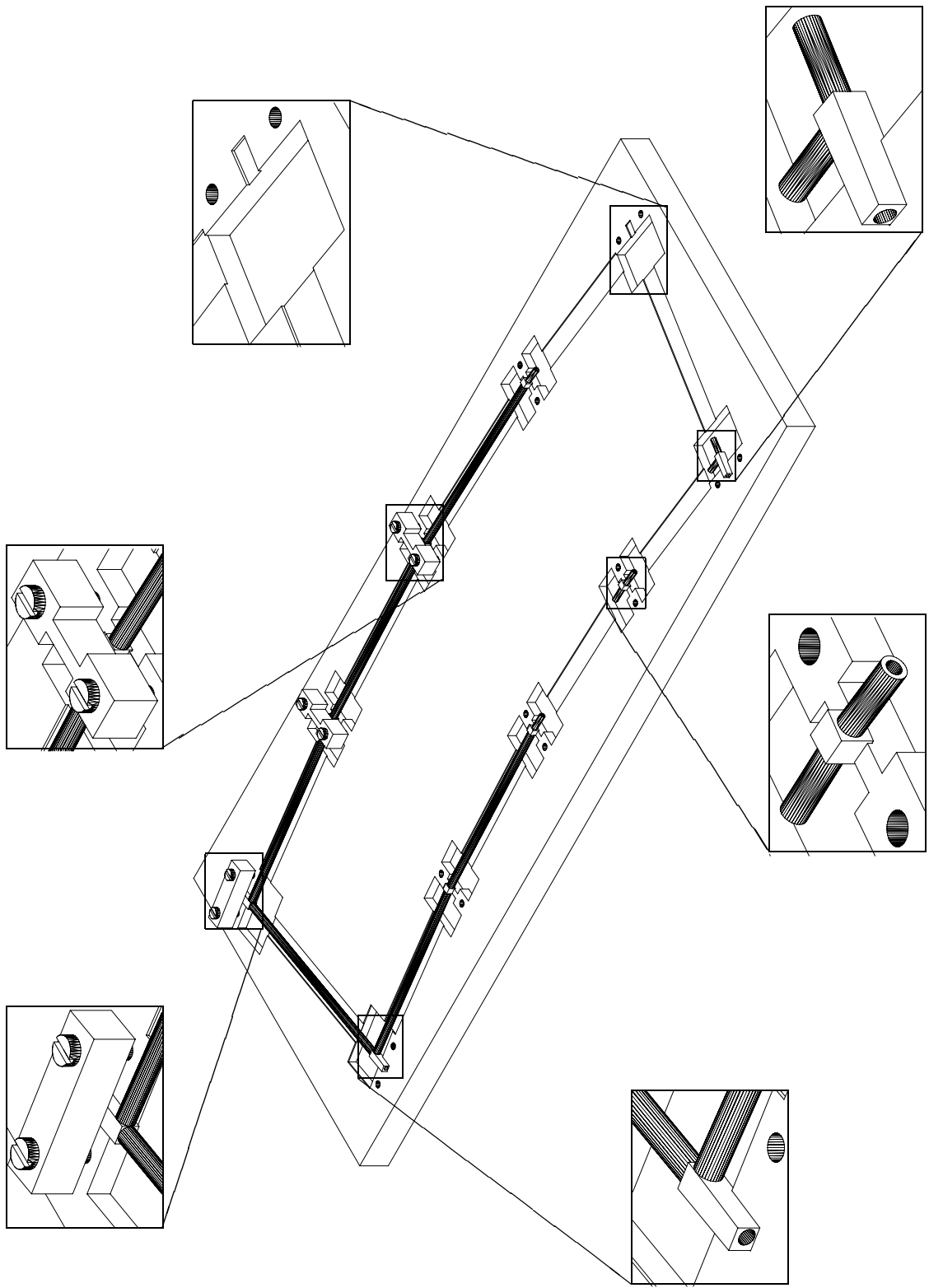


Figure 1: MSGC gluing jig with partly mounted module frame.

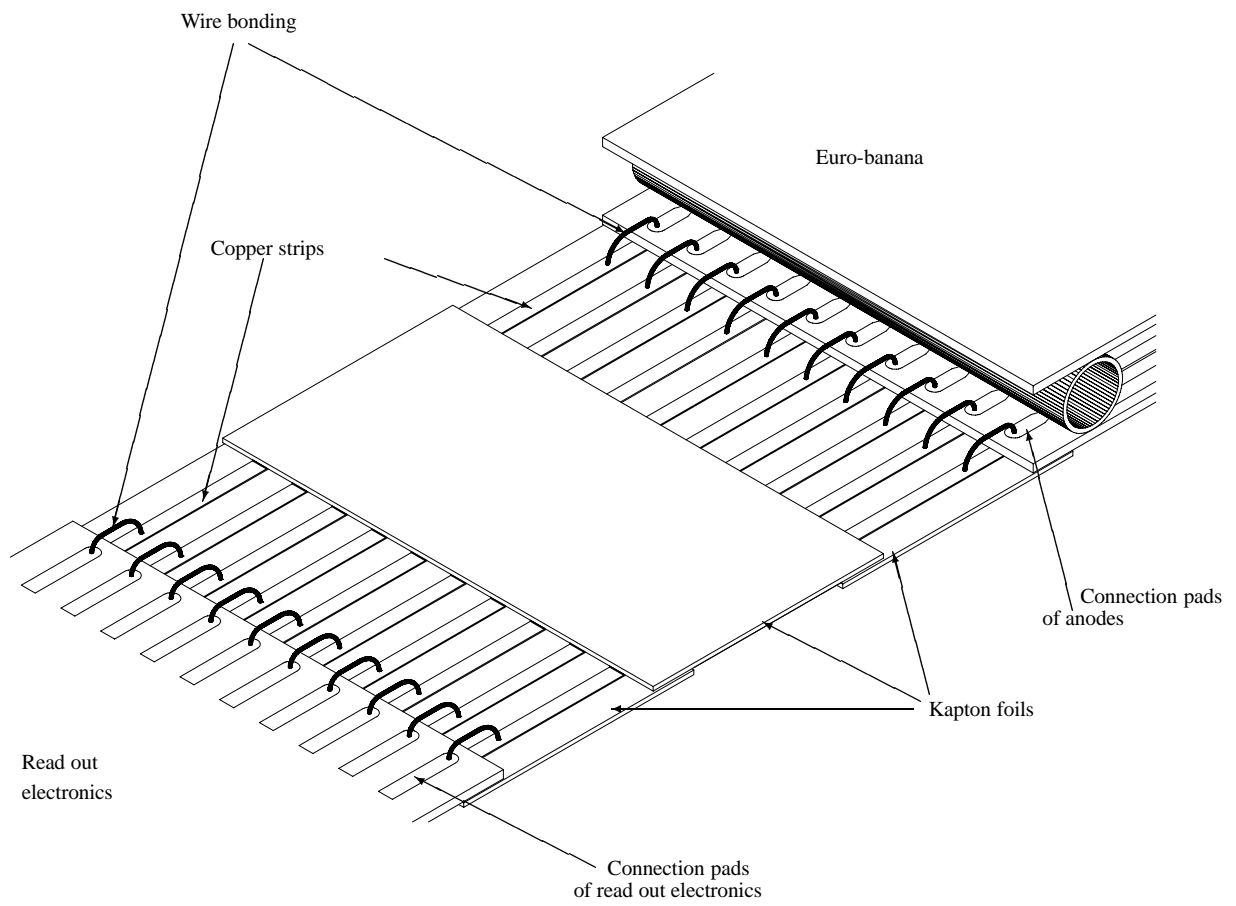


Figure 2: *Connections using anisotropic conductive glue.*



Detector module *Euro-banana*

Scintillators

Silicon Telescope

Scintillator

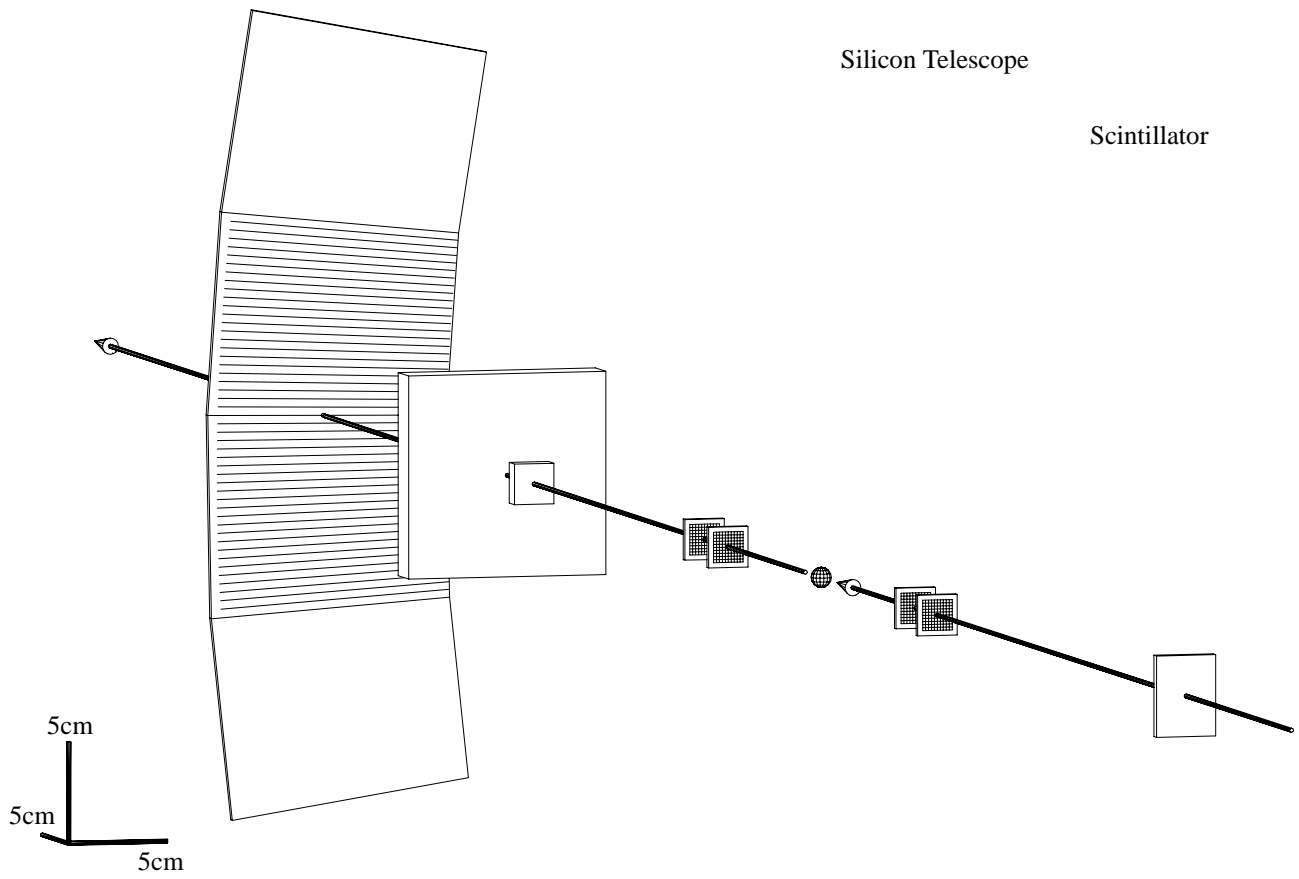


Figure 3: *Test beam set up.*

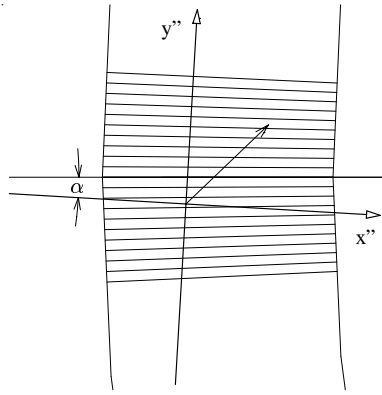


Figure 4: *Rotation of coordinate system.*

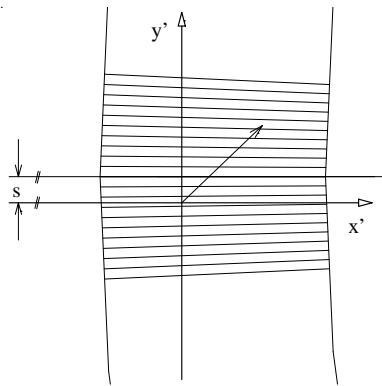


Figure 5: *Translation of coordinate system.*

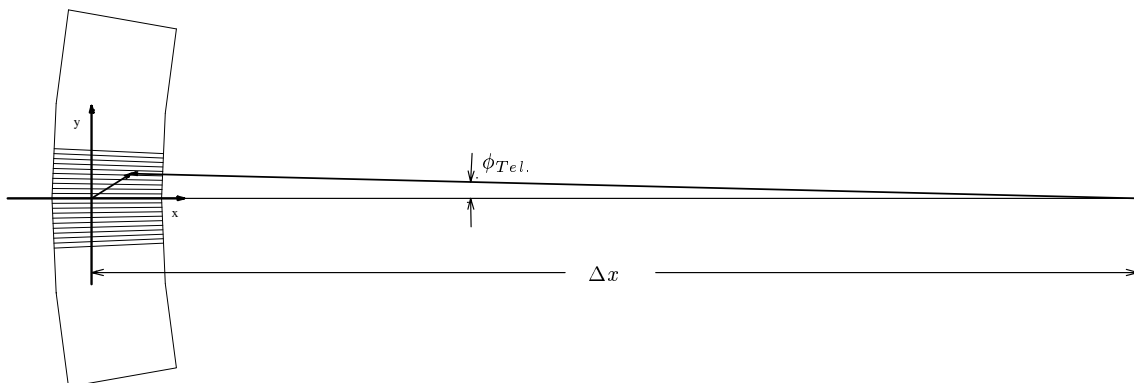
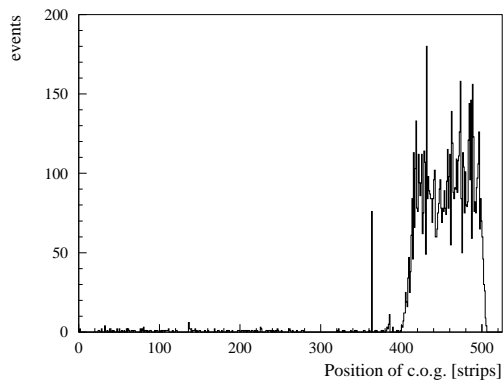
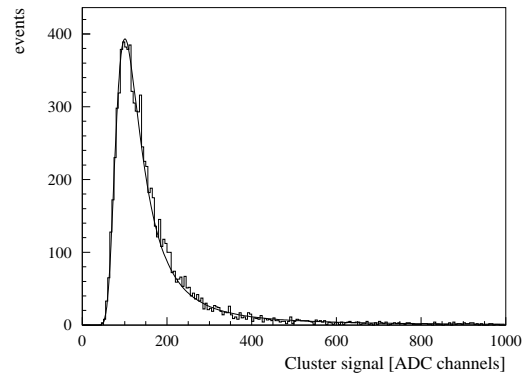


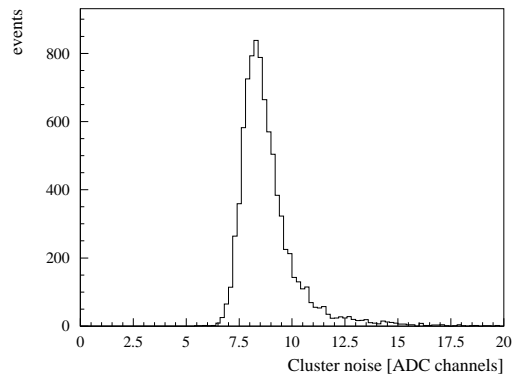
Figure 6: *Final coordinate system*



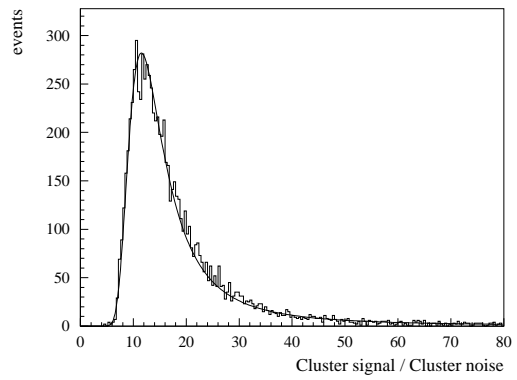
a)



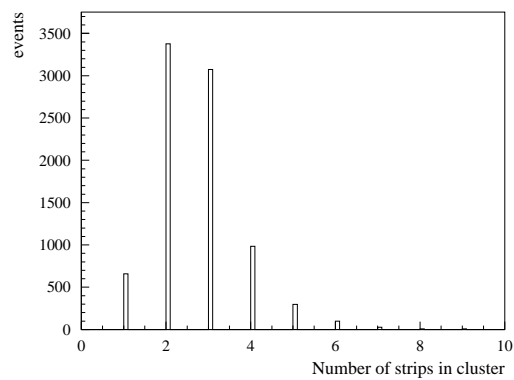
b)



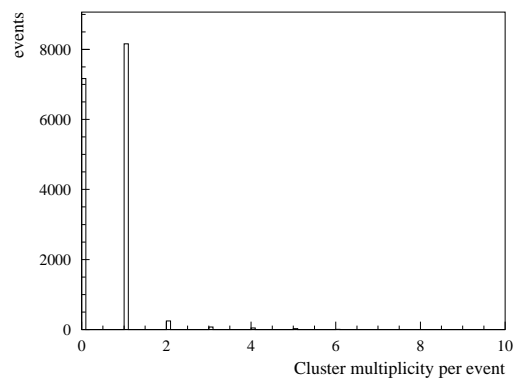
c)



d)



e)



f)

Figure 7: Typical response.

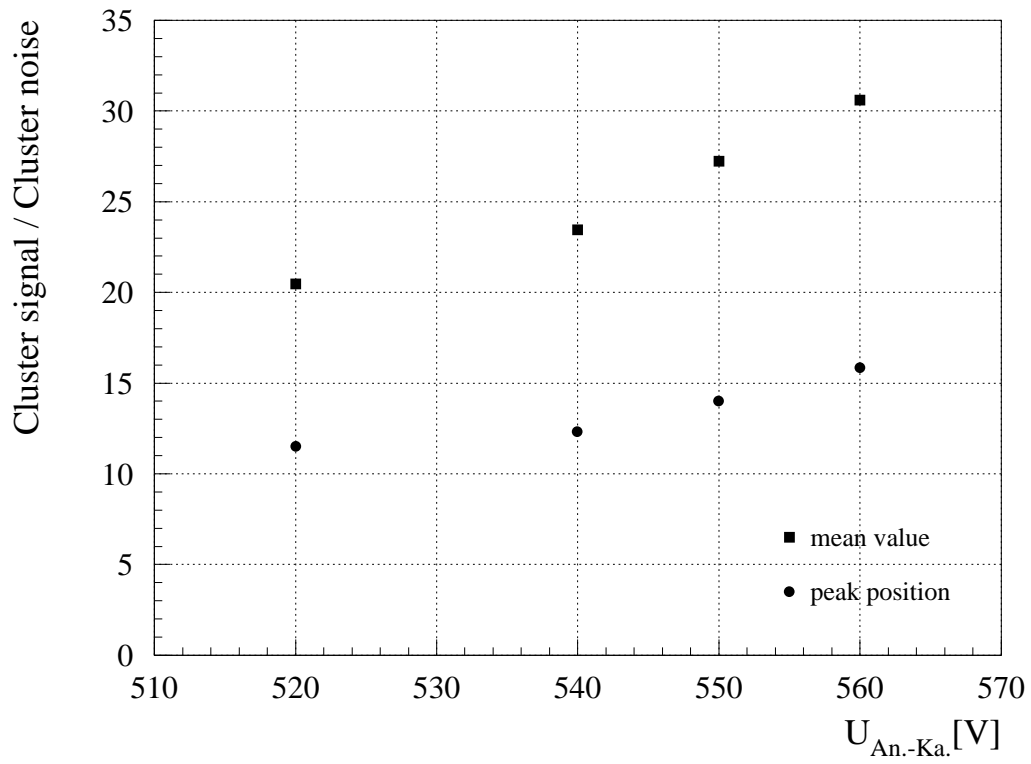
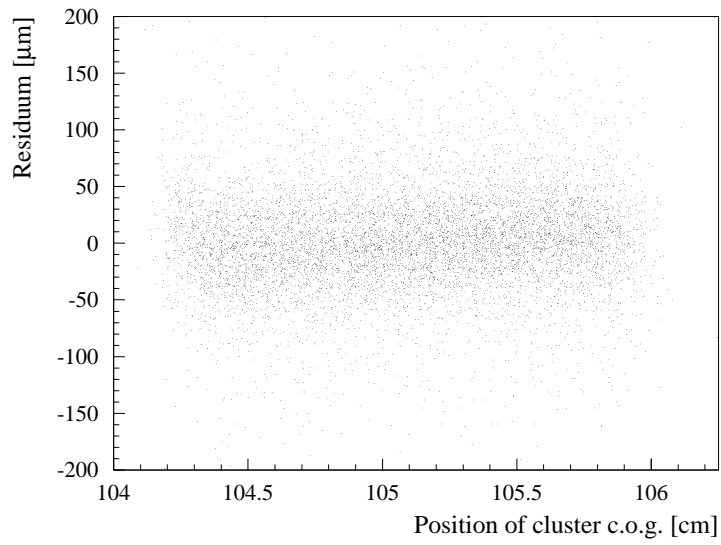
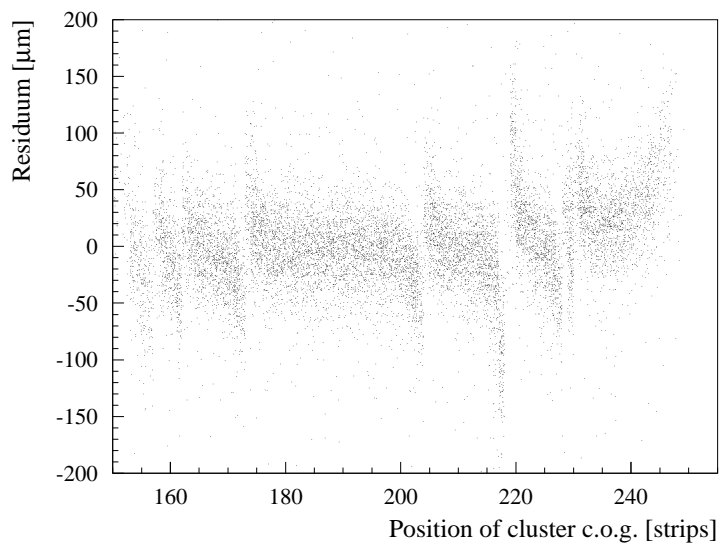


Figure 8: Bias voltage scan of signal to noise ratio.

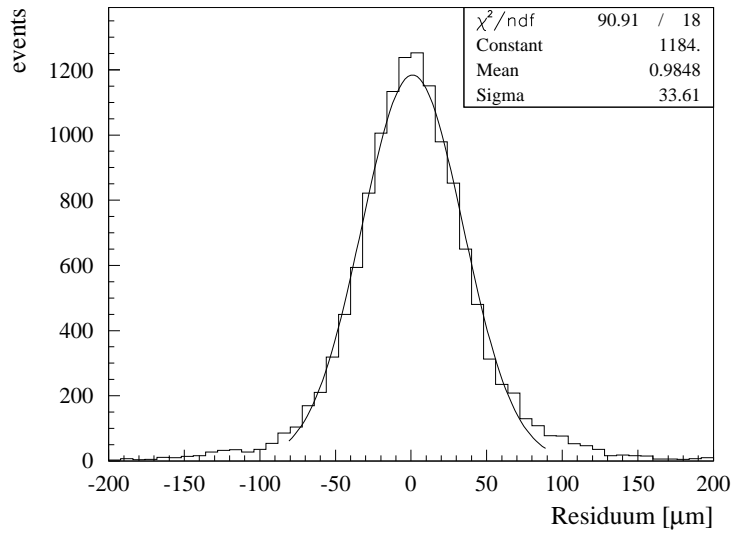


a)

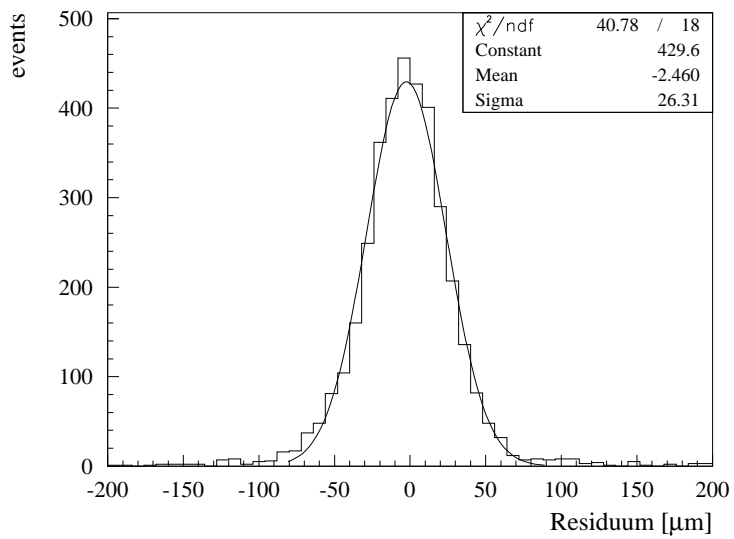


b)

Figure 9: *Residual as a function of cluster position.*



a)



b)

Figure 10: *Distribution of residual.*

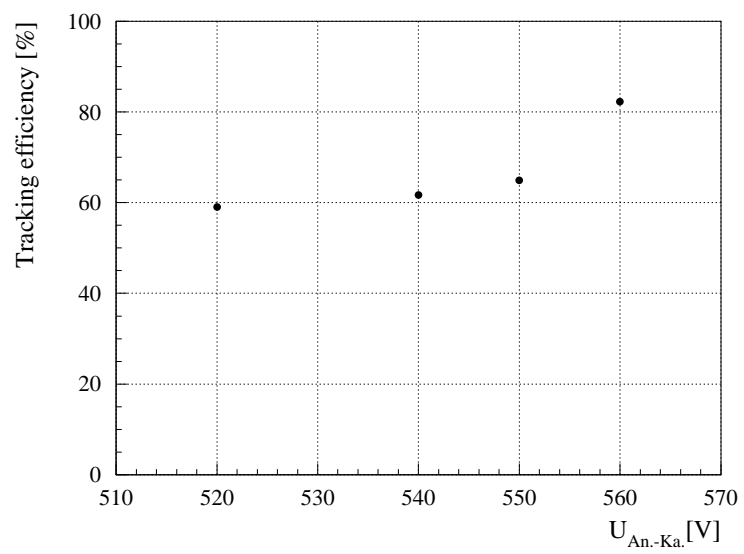


Figure 11: *Tracking efficiency as a function of bias voltage.*